

JRDB: A Dataset and Benchmark for Visual Perception for Navigation in Human Environments

Roberto Martín-Martín*, Hamid Rezatofghi*, Abhijeet Shenoi, Mihir Patel, JunYoung Gwak, Nathan Dass, Alan Federman, Patrick Goebel, Silvio Savarese

Abstract—We present JRDB, a novel dataset collected from our social mobile manipulator JackRabbit. The dataset includes 64 minutes of multimodal sensor data including stereo cylindrical 360 °RGB video at 15 fps, 3D point clouds from two Velodyne 16 Lidars, line 3D point clouds from two Sick Lidars, audio signal, RGBD video at 30 fps, 360°spherical image from a fisheye camera and encoder values from the robot's wheels. Our dataset includes data from traditionally underrepresented scenes such as indoor environments and pedestrian areas, from both stationary and navigating robot platform. The dataset has been annotated with over 2.3 million bounding boxes spread over 5 individual cameras and 1.8 million associated 3D cuboids around all people in the scenes totalling over 3500 time consistent trajectories. Together with our dataset and the annotations, we launch a benchmark and metrics for 2D and 3D person detection and tracking. With this dataset, that we plan on further annotating in the future, we hope to provide a new source of data and a test-bench for research in the areas of robot autonomous navigation and all perceptual tasks around social robotics in human environments.

Index Terms—Robot Navigation, Social Robotics, Person Detection, Person Tracking

1 INTRODUCTION

IN the recent past, the computer vision and robotics communities have proposed several centralized benchmarks to evaluate and compare different machine visual perception solutions. The tasks evaluated include a) scene understanding problems, *e.g.* object detection [1], [2], semantic and instance segmentation [1], [2], [3], 3D reconstruction [4], optical flow computation [5], and stereo estimation [6], and b) problems related to understanding, analyzing and predicting human motion and behaviour, *e.g.* pedestrian detection and tracking [7], [8], [9], human pose estimation [10] and human activity understanding [11]. Despite potential pitfalls of such benchmarks, they have proven to be extremely helpful to advance the state-of-the-art in the respective research fields.

However, existing benchmarks mainly focus on the one or few visual perception tasks defined on single RGB images [1], [2], [12] or RGB video sequences [3], [9], [10], [11]. With the rise of popularity of 3D sensory data systems based on LiDAR, some benchmarks have begun to provide both 2D and 3D sensor data, and to define new scene understanding tasks on this geometric information. Some examples of these datasets are KITTI [7], Apolloscape [13] and Oxford's Robotic Car [14]. Nonetheless, their targeted domain application is autonomous driving: the data they provide is captured exclusively from sensor suites on top of cars and the data only depicts streets, roads and highways.

In this paper, we target a unique visual domain tailored to the perceptual tasks related to navigation in **human environments**, both **indoors** and **outdoors**. We hope that this new domain provide the community an opportunity to develop visual perception

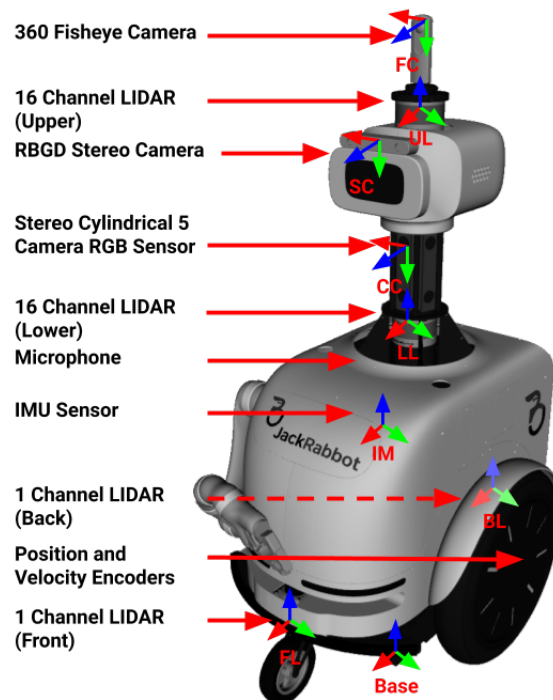


Fig. 1: JackRabbit, our data collection platform, is equipped with 4 LIDAR sensors, 3 cameras, 2 movement encoders, an IMU sensor, and a microphone.

- * indicates equal contribution.
- All the authors are with the Stanford Vision and Learning Laboratory, Stanford University, USA
- E-mail: [robertom, hamidrt, ashenoj, mihirp, jgwak, pgoebel, ssilvio]@cs.stanford.edu

frameworks for various types of autonomous navigation agents, not only self-driving cars but also other types of agents like social

mobile robots¹. These agents require to understand both indoor and outdoor scenes in order to interact successfully with humans, predict their behaviour in these environments, and incorporate this behavior in agent’s planning and decision processes.

With this motivation, we present a new dataset, the **JackRabbit social navigation dataset**, and several visual benchmarks associated to it. Our dataset contains **64** minutes of sensor data acquired from our mobile robot JackRabbit² comprising **54** sequences indoors and outdoors in a university campus environment. The sensor data includes stereo RGB 360° cylindrical video streams, continuous 3D point clouds from two LiDAR sensors, audio and GPS sensing. Currently for this first phase, we provide the following ground truth annotations for our captured data³: a) 2D bounding boxes in each camera and the cylindrical images for human/pedestrian class, b) an occlusion attributes for each 2D bounding box, c) 3D oriented bounding boxes from LiDAR data for human/pedestrian class, d) an association link between 2D and 3D bounding boxes c) time consistent trajectories (tracks) for all annotated persons in both 2D and 3D. Using the current annotations, we will provide a unified and standardized benchmark for 2D-3D person detection and tracking.

2 SENSOR SETUP: THE JACKRABBIT PLATFORM

We collected our multimodal dataset with the sensors on-board of our mobile-manipulator JackRabbit (see Fig. 1). JackRabbit (JR) is a custom-design robot platform tailored to navigate and interact in human environments. On the actuation side, JR is composed of a Segway two active wheeled based, with two passive caster wheels for stability, and a 6 degrees-of-freedom Kinova Mico arm with two-fingered end-effector. The head of the robot is equipped with a LCD display that renders different facial expressions to engage with humans and communicate intentions. The display is actively moved by two Maxon motors providing pan-tilt control.

The JackRabbit platform is equipped with multiple visual, audio, depth and motion sensors, as shown in Fig. 1. In the following we list the most relevant sensor properties.

- 2 × Velodyne 16 Puck LITE rotating 3D laser scanner, 10 Hz, 16 beams, 0.09 degree angular resolution, 2 cm distance accuracy, collecting approx. 1.3 million points/second, field of view: 360° horizontal, 26.8° vertical, range: 100 m
- 2 × SICK rotating 3D laser scanner
- Occam cylindrical stereo sensor suite composed of two rows of five RGB cameras each. Each individual camera has a resolution of 752 × 480
- Microphone x
- Ricoh Theta 360° fisheye camera
- ZED RGBD stereo camera
- Position encoders on each of the active wheels of the base of resolution

JackRabbit is also equipped with an onboard computational unit including two GPUs. The onboard computer runs Linux 16.04 and ROS (Robot Operating System) Kinetic that we use to collect multimodal synchronized signals in the form of rosbags.

1. In 2030 up to 20% of the jobs in retail (including malls, restocking, last-mile delivery, guidance, etc.) could be carried out by social robots navigation among humans [15]

2. <http://svl.stanford.edu/projects/jackrabbit/>

3. In near future, we have plans to augment with other types of annotations for many other visual perception tasks, e.g. 2D human skeleton pose and individual, group and social activity labels.

3 CAPTURED DATA

We collect time synchronized data from all sensors and save it on the on-board computer. The data is recorded from 30 different locations indoors and outdoors, all in a university campus environment, with varying and uncontrolled environmental conditions such as illumination and other natural and dynamical elements. We also ensure the recorded data captures a variation of natural human posture, behaviour and social activities in different crowd densities in indoor and outdoor environments. Furthermore, to incorporate a diversity in the robot’s ego-motion, we use a combination of static and moving sensor (robot) views to capture the data.

The JackRabbit dataset includes 54 sensor sequences captured from the multimodal robot’s sensor stream containing:

- Video streams at 15 fps from stereo cylindrical 360° RGB cameras
- Continuous 3D point clouds from 2 velodyne LiDAR signals of 16 planar rays
- RGBD video streams at 30 fps,
- 360° spherical image from a fisheye camera,
- Line 3D point clouds from two Sick LiDARs,
- Audio signal,
- Encoder values from the robot’s wheels.

3.1 360 Cylindrical Panorama Stitching

The individual cameras (5 in total) are pinhole cameras, each of size 752 × 480. To stitch them into a single 360° cylindrical, RGB image, we adopt the following procedure. We first construct a mapping from pixels in the cylindrical image to pixels in the individual cameras. To do so, every pixel, say (x, y) in the cylindrical image is assumed to be at some constant distance r from the camera center. This allows us to obtain this point’s 3D coordinates, given by $(r \cos \theta, y, r \sin \theta)$, where θ is the angle made by the line passing through the origin and the 3D point, with the positive X axis of the base frame. Given this world point, we project it onto each of the five individual cameras by using the extrinsic parameters R and T , the intrinsic parameters K , and the distortion coefficients D . The projected point (\hat{x}, \hat{y}) is given by:

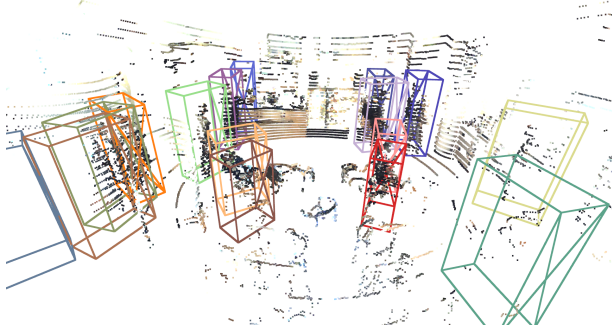
$$\begin{pmatrix} \hat{x} \\ \hat{y} \end{pmatrix} = K f_D \left([R \quad T] \begin{pmatrix} r \cos \theta \\ y \\ r \sin \theta \\ 1 \end{pmatrix} \right)$$

where f_D is the distortion function, which is parametrised by the distortion coefficients D . To eliminate cases where the point is behind the camera onto which we are projecting, we first calculate

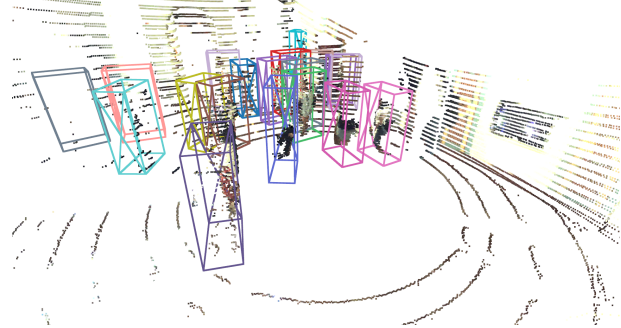
$$\begin{pmatrix} x' \\ y' \\ z' \end{pmatrix} = [R \quad T] \begin{pmatrix} r \cos \theta \\ y \\ r \sin \theta \\ 1 \end{pmatrix}$$

If z' is less than 0, we ignore this correspondence. We also eliminate correspondences beyond the bounds of the individual images (\hat{x} or \hat{y} lie outside the image). Hence, we obtain point correspondences between (x, y) and (\hat{x}, \hat{y}) for the individual cameras. Given these correspondences, we perform a mapping followed by smoothing of the individual images onto a cylindrical surface, resulting in the 360° RGB image. This stitching is implemented in the camera driver.

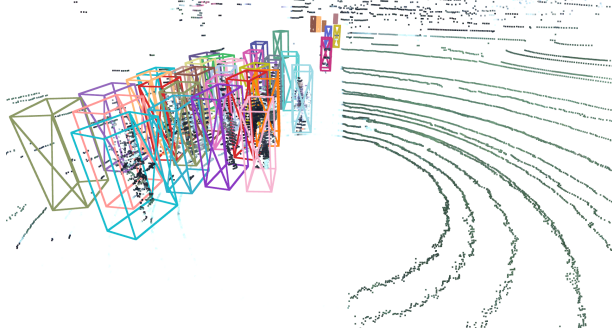
Fig 2 demonstrates some examples of the captured data from the perspective of 360° cylindrical panorama camera and point cloud data.



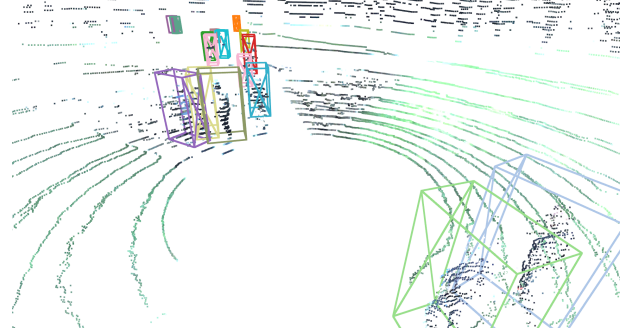
(a) *bytes-cafe-2019-02-07_0*: Stationary robot at indoor scene.



(b) *cubberly-auditorium-2019-04-22_0*: Moving robot at indoor scene.



(c) *huang-lane-2019-02-12_0*: Stationary robot at outdoor scene.



(d) *memorial-court-2019-03-16_0*: Moving robot at outdoor scene.

Fig. 2: Sample visualization of the dataset. For each subfigure, top: 2D stitched 360° panorama with human-annotated 2D bounding boxes, bottom: 3D Velodyne point clouds with human-annotated 3D rotated bounding boxes. In order to demonstrate the accuracy of camera registration, we visualize 3D point clouds with color extracted from the projected 2D RGB stitched 360 panorama image. Our dataset captures a variety of pedestrian density, indoor/outdoor scenes, and moving/stationary robot.

4 ANNOTATIONS

We annotate all pedestrians in 2D stereo images and 3D point clouds with 2D and 3D bounding boxes accordingly. Additionally, we label all persons in the scene with a unique ID that is consistent across 2D and 3D annotation within the same sequence. Such bounding box annotations allow us to train and evaluate various interesting tasks, which we will discuss in section 5. In the following subsections, we will discuss the details of the annotation such as bounding box parameterization and other metadata.

4.1 2D Bounding Box Annotation

We annotate a 2D bounding box alongside with some metadata for each person in each of the five images as following.

- *label_id*: Unique ID of the person that is consistent across 2D and 3D annotation within the same sequence
- *box*: 2D bounding box parameterized as (x, y) location of the upper left corner of the bounding box and (w, h) size of the bounding box
- *truncated*: Flag indicating whether the object is leaving the upper or lower border of the image boundary. Please note that the annotation is on 360° stitched panorama and horizontal truncation is not possible.

- *occlusion*: Level of occlusion of the pedestrian in the image. We consider the following four levels: *Fully_visible* (no occlusion), *Mostly_visible* (more than 50% visible), *Severely_occluded* (more than 50% occluded), *Fully_occluded* (not visible at all).
- *interpolated*: Flag indicating whether this labels were direct products of the human annotation (at 7 fps) or generated by the interpolation of labeled frames (at 15 fps).
- *no_eval*: Flag that indicates if the annotation does not fulfill all the conditions to be included in the evaluation of a detector/tracker as described in Sec. 5.
- *area*: Area of the bounding box.

Stitching 2D annotations for 360 panorama image: We also merge the annotations from the five images into the stitched 360° panorama image using the similar procedure discussed in section 3.1. To this end, we first project the coordinates of four corners of bounding box to 360° panorama image and then fit the tightest enclosing axis-aligned rectangle for those corners. For the cases when a person, seen in more than one view, has a bounding box annotated in more than one camera, we have ensured that their IDs are consistent during the annotation phase in each camera. Therefore, during merging process, we simply fit the tightest bounding box on all projected corners with the same

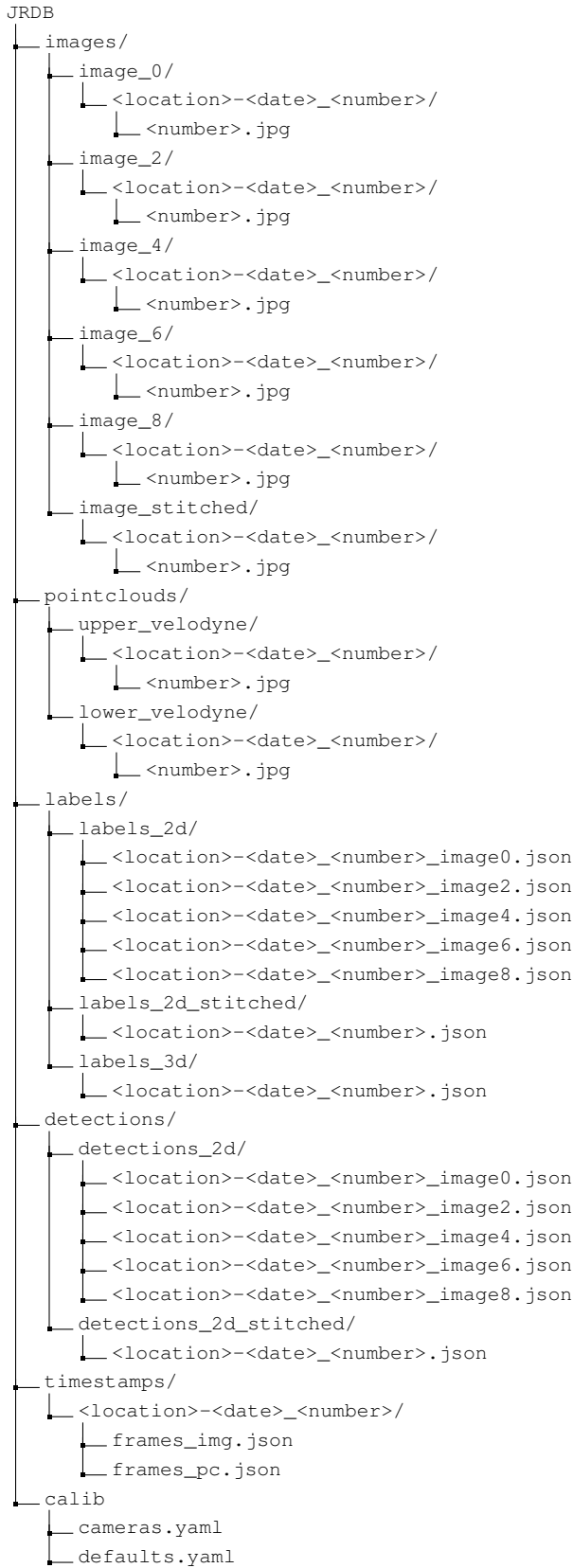


Fig. 3: The dataset contains image and pointcloud data, along with labels, sample detections, timestamps and calibration information. Further detail is in text.

ID. In cases where an ID is split between the right extreme and left extreme of the cylindrical image, we adopt the convention of coordinates indicating the top left of the box and extending beyond the right edge of the image.

The resulting stitched annotation is the a 2D bounding box for each person in each frame of the stitched images (Fig 2).

4.2 3D Bounding Box Annotation

We annotate a 3D bounding box alongside with some metadata for each pedestrian in the Velodyne point clouds as following.

- *label_id*: Unique ID of the pedestrian that is consistent across 2D and 3D annotation within the same sequence
- *box*: 3D bounding box parameterized as (cx, cy, cz) location of the center of the cuboid, (h, w, l) size of the bounding box, and *rot_z* rotation angle around the gravity (*z*) axis.
- *interpolated*: Flag indicating whether this labels were direct products of the human annotation (at 7 fps) or generated by the interpolation of labeled frames (at 15 fps).
- *num_points*: Number of points that lies within the 3D bounding box.
- *distance*: Distance from the sensors to the people.
- *no_eval*: Flag that indicates if the annotation does not fulfill all the conditions to be included in the evaluation of a detector/tracker as described in 5.
- *observation_angle*: Rotation angle in radians defined as $\tan^{-1}(\frac{-y}{x})$ for a point with x-coordinate *x* and y-coordinate *y*.

4.3 Data Split and The Statistics

In order to provide a benchmark data, we divided the 54 captured sequences into train and test splits equally. We considered that the same number of indoor and outdoor sequences captured using stationary or moving robot appears in each split. Moreover, we ensured that the train and test splits contain very diverse scenes while following a comparably very similar annotation statistics (See Tab. 1 and Fig. 4-7). All relevant captured data, *i.e.* point cloud streams, 5 stereos camera images as well as 360°panorama stitched images for both train and test split⁴ and annotations for the train set are publicly available to download at <https://jrdb.stanford.edu>.

5 BENCHMARKS AND METRICS

Based on our associated annotations in RGB images and LiDAR pointclouds, we propose the following four benchmarks:

- 2D person detection (in images)
- 3D person detection
- 2D person tracking (in images)
- 3D person tracking

Participants are free to use any of the available sensor modalities for each of the tasks, e.g. they can use RGB images and 3D point clouds for 2D person detection or for 3D person tracking.

In the following we describe the evaluation criteria and metrics we use for detection and tracking.

4. Excluding 5.2 sec from each test sequence which are not publicly released for future forecasting benchmarks

Data Split	Train Set			Test Set		
	Indoor	Outdoor	Total	Indoor	Outdoor	Total
Number of sequences	17	10	27	16	11	27
Number of frames	19248	8699	27947	17408	12359	29767
Number of 2D Boxes	765 K	324 K	1.08 M	868 K	405 K	1.27 M
Number of 2D tracks	1229	564	1793	1201	617	1818
Avg. track length in frames (2D)	475.7	457.8	470.0	567.9	534.3	556.5
Number of 3D Boxes	578 K	254 K	832 K	671 K	324 K	995K
Number of 3D tracks	1220	554	1774	1186	611	1797
Avg. track length in frames (3D)	473.7	459.3	469.2	566.1	529.9	553.8

TABLE 1: Table summarizing various statistics of the dataset. All 2D statistics are reported as an aggregate of the 5 individual cameras used to construct the 360° cylindrical RGB image. Test set statistics above include the last 5.2s of each sequence in the test set which are not publicly released, for future construction of a trajectory prediction benchmark. We aimed to have near identical distributions between the train and test splits.

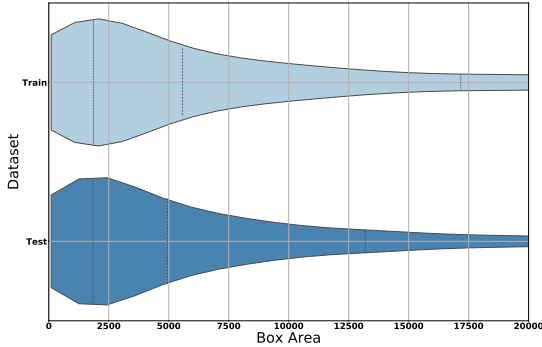


Fig. 4: A violin plot showing a Kernel Density Estimate of the area of bounding boxes for the train and test split of the dataset. The quartiles are shown as dotted lines in the figure.

5.1 Person Detection

We evaluate 2D and 3D detection performance using the mean Average Precision (mAP) metric. A prediction is considered true positive if the IoU between the prediction and the ground-truth bounding box is over 0.5. Then, we take average of 11-point interpolated precision to compute mean average precision, just as in Pascal VOC2008 [16]. Here is a mathematical definition of mAP.

$$mAP = \frac{1}{11} \sum_{r \in \{0, 0.1, \dots, 1\}} \max_{\tilde{r}: \tilde{r} \geq r} Precision(\tilde{r})$$

where $Precision(r)$ is the measured precision at recall r . We use the implementation of mAP evaluator of KITTI object detection benchmark [17]. Only those bounding boxes which are greater 500 pixel² in area are considered for the 2D detection benchmark, and only those 3D boxes that are within 25m of the sensor are considered for the 3D detection benchmark.

5.2 Person Tracking

We evaluate 2D and 3D tracking performance using the Clear-MOT metrics [18]. These metrics are multiple object tracking accuracy (MOTA) and multiple object tracking precision (MOTP). Mathematically, MOTA is defined as

$$MOTA = 1 - \frac{\sum_t (FN_t + FP_t + ID_t)}{\sum_t GT_t}$$

where FN_t, FP_t, ID_t, GT_t are false negatives, false positives, id switches, and ground truth at frame t respectively. MOTP is defined as

$$MOTP = \frac{\sum_{t,i} d_{t,i}}{\sum_t c_t}$$

where $d_{t,i}, c_t$ are the intersection over union for the i th match and the count of matches made at frame t respectively.

To evaluate 2D tracking, we run Clear-MOT metrics using an IoU threshold of 0.5. To evaluate 3D tracking, the 3D IoU is calculated using a combination of the Sutherland-Hodgman algorithm [19] and the shoelace formula (surveyor’s formula) to determine the area of intersection. The Sutherland Hodgman algorithm is an algorithm used to clip polygons. Given the subject polygon $P1$ and a convex polygon $P2$, it extends each line segment of $P2$ to clip the edges of $P1$, i.e., the edges of $P1$ are restricted to fall within $P2$. The resulting clipped polygon represents the area of intersection. Given the set of vertices of this polygon, sorted in clockwise order, we apply the shoelace formula to find its area. The shoelace formula is given by:

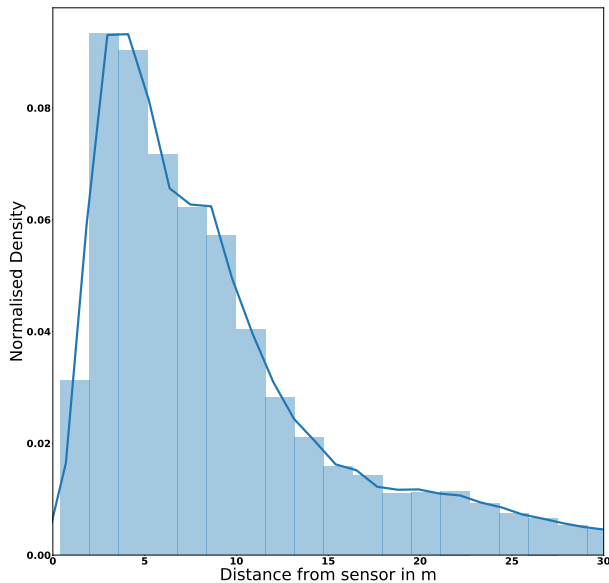
$$A = \frac{1}{2} \left| \sum_{i=1}^{n-1} x_i y_{i+1} + x_n y_1 - \sum_{i=1}^{n-1} x_{i+1} y_i - x_1 y_n \right|$$

where A is the area of the polygon with n vertices $(x_1, y_1), (x_2, y_2) \dots (x_n, y_n)$. An 3D-IoU threshold of 0.3 is used to determine matches.

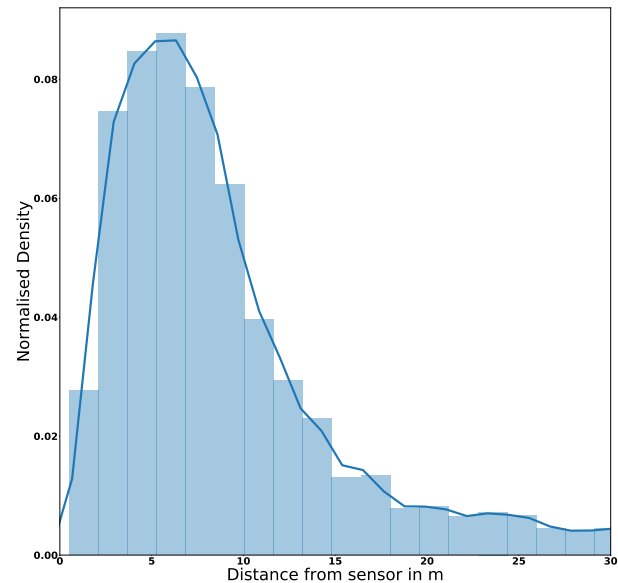
For both 2D and 3D tracking, we only evaluate objects from the first frame in which they are fully visible, until the last frame that they are fully visible before either i) being completely occluded for the rest of the lifetime of that track or ii) leaving the scene. Occlusion in 2D is taken to mean visual occlusion. For 3D tracking, occlusion instead implies that the object position cannot reasonably be determined. Therefore when an object has less than 10 points within its 3D bounding box, we assume the object is occluded in 3D. The 2D and 3D evaluations differ only in their calculations of IoU, the IoU threshold used to determine matches and the definition of occlusion.

6 CONCLUSION AND FUTURE WORK

We presented JRDB, a novel dataset containing multimodal streams acquired in human environments: university indoor buildings and pedestrian areas on campus. The dataset of temporally synchronized and calibrated data includes images from 360° stereo cylindrical cameras, LiDAR 3D point clouds, audio signals, IMU values and



(a) Training Set Distribution



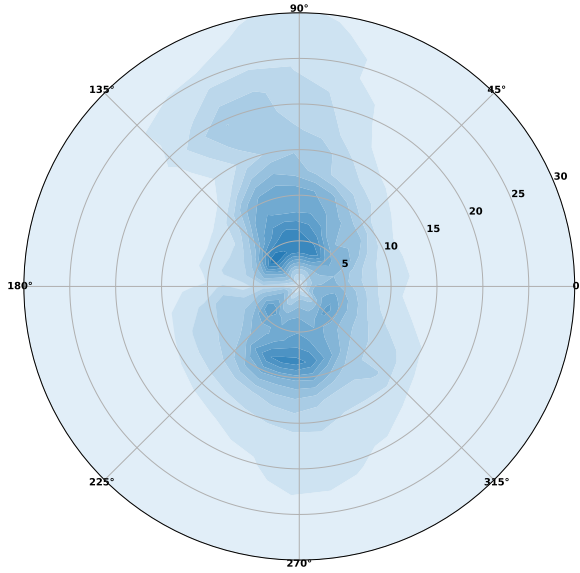
(b) Test Set Distribution

Fig. 5: The distribution of distances of 3D bounding boxes of people remains relatively unchanged between training and test sets. Our dataset contains a large number of frames of indoor scenes where people tend to be closer to the robot, resulting in a distribution with a mode at approximately 5m, for both train and test splits. The long-tailed nature of the distribution is a consequence of the outdoor scenes, with some annotations as far as 80m from JackRabbit.

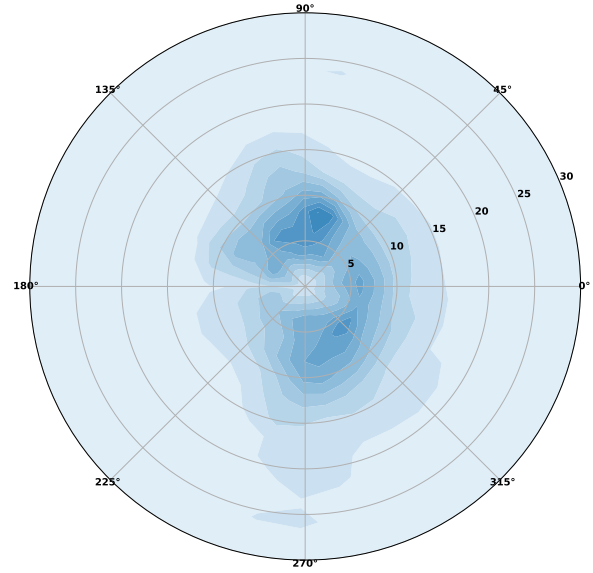
encoder readings from the robot’s base. The data includes scenes where the robot navigates among humans. The dataset has been annotated with ground truth 2D bounding boxes and associated 3D cuboids around all persons in the scenes. We expect this dataset to support research in perception for autonomous agents in human and social contexts. Our future plans include continue annotating ground truth values for individual and group activities, social grouping, and human posture.

REFERENCES

- [1] M. Everingham, L. Van Gool, C. Williams, J. Winn, and A. Zisserman, *The PASCAL Visual Object Classes Challenge 2012 (VOC2012) Results*, 2012. [Online]. Available: <http://www.pascal-network.org/challenges/VOC/voc2012/workshop/index.html>
- [2] T.-Y. Lin, M. Maire, S. Belongie, J. Hays, P. Perona, D. Ramanan, P. Dollar, and C. L. Zitnick, “Microsoft coco: Common objects in context,” *ECCV*, 2014.
- [3] M. Cordts, M. Omran, S. Ramos, T. Rehfeld, M. Enzweiler, R. Benenson, U. Franke, S. Roth, and B. Schiele, “The cityscapes dataset for semantic urban scene understanding,” in *CVPR*, 2016, pp. 3213–3223.
- [4] S. M. Seitz, B. Curless, J. Diebel, D. Scharstein, and R. Szeliski, “A comparison and evaluation of multi-view stereo reconstruction algorithms,” pp. 519–528.
- [5] S. Baker, D. Scharstein, J. P. Lewis, S. Roth, M. J. Black, and R. Szeliski, “A database and evaluation methodology for optical flow,” vol. 92, no. 1, pp. 1–31, Mar. 2011. [Online]. Available: <http://vision.middlebury.edu/flow/floweval-ijcv2011.pdf>
- [6] D. Scharstein and R. Szeliski, “A taxonomy and evaluation of dense two-frame stereo correspondence algorithms,” vol. 47, no. 1-3, pp. 7–42, Apr. 2002. [Online]. Available: <http://link.springer.com/article/10.1023/A%3A1014573219977>
- [7] A. Geiger, P. Lenz, and R. Urtasun, “Are we ready for autonomous driving? The KITTI Vision Benchmark Suite.” [Online]. Available: <http://www.cvlibs.net/publications/cvpr12.pdf>
- [8] L. Leal-Taixé, A. Milan, I. Reid, S. Roth, and K. Schindler, “MOTChallenge 2015: Towards a benchmark for multi-target tracking,” *arXiv:1504.01942*, 2015.
- [9] A. Milan, L. Leal-Taixé, I. Reid, S. Roth, and K. Schindler, “MOTChallenge 2016: Annotation and evaluation,” *arXiv:1603.00831*, 2016.
- [10] M. Andriluka, U. Iqbal, E. Insafutdinov, L. Pishchulin, A. Milan, J. Gall, and B. Schiele, “PoseTrack: A benchmark for human pose estimation and tracking,” in *CVPR*, 2018, pp. 5167–5176.
- [11] F. Caba Heilbron, V. Escorcia, B. Ghanem, and J. Carlos Niebles, “Activi-tynet: A large-scale video benchmark for human activity understanding,” in *CVPR*, 2015, pp. 961–970.
- [12] O. Russakovsky, J. Deng, H. Su, J. Krause, S. Satheesh, S. Ma, Z. Huang, A. Karpathy, A. Khosla, M. Bernstein, A. C. Berg, and L. Fei-Fei., “Imagenet large scale visual recognition challenge,” *IJCV*, 2015.
- [13] X. Huang, X. Cheng, Q. Geng, B. Cao, D. Zhou, P. Wang, Y. Lin, and R. Yang, “The apolloscape dataset for autonomous driving,” in *Proceedings of the IEEE Conference on Computer Vision and Pattern Recognition Workshops*, 2018, pp. 954–960.
- [14] W. Maddern, G. Pascoe, C. Linegar, and P. Newman, “1 Year, 1000km: The Oxford RobotCar Dataset,” *The International Journal of Robotics Research (IJRR)*, vol. 36, no. 1, pp. 3–15, 2017. [Online]. Available: <http://dx.doi.org/10.1177/0278364916679498>
- [15] J. Manyika, S. Lund, M. Chui, J. Bughin, J. Woetzel, P. Batra, R. Ko, and S. Sanghvi, “Jobs lost, jobs gained: Workforce transitions in a time of automation,” *McKinsey Global Institute*, 2017.
- [16] M. Everingham, L. Van Gool, C. K. I. Williams, J. Winn, and A. Zisserman, “The PASCAL Visual Object Classes Challenge 2008 (VOC2008) Results,” <http://www.pascal-network.org/challenges/VOC/voc2008/workshop/index.html>.
- [17] A. Geiger, P. Lenz, and R. Urtasun, “Are we ready for autonomous driving? the kitti vision benchmark suite,” in *Conference on Computer Vision and Pattern Recognition (CVPR)*, 2012.
- [18] K. Bernardin and R. Stiefelhagen, “Evaluating multiple object tracking performance: the clear mot metrics,” *Journal on Image and Video Processing*, vol. 2008, p. 1, 2008.
- [19] I. E. Sutherland and G. W. Hodgman, “Reentrant polygon clipping,” *Communications of the ACM*, vol. 17, no. 1, pp. 32–42, 1974.

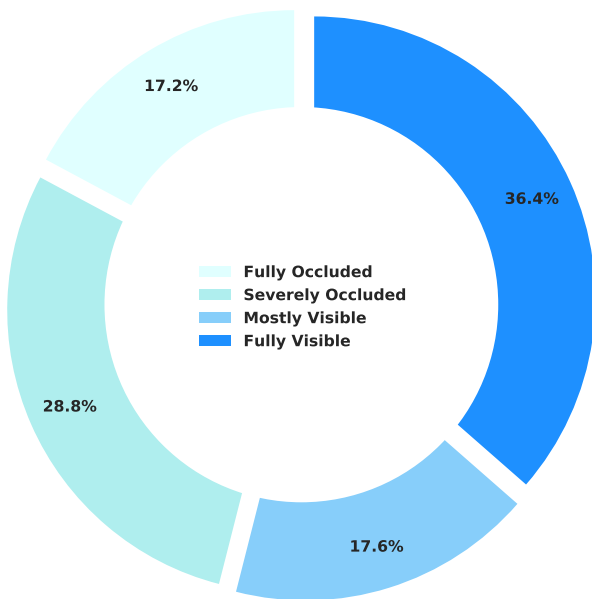


(a) Training Set Kernel Density Estimate

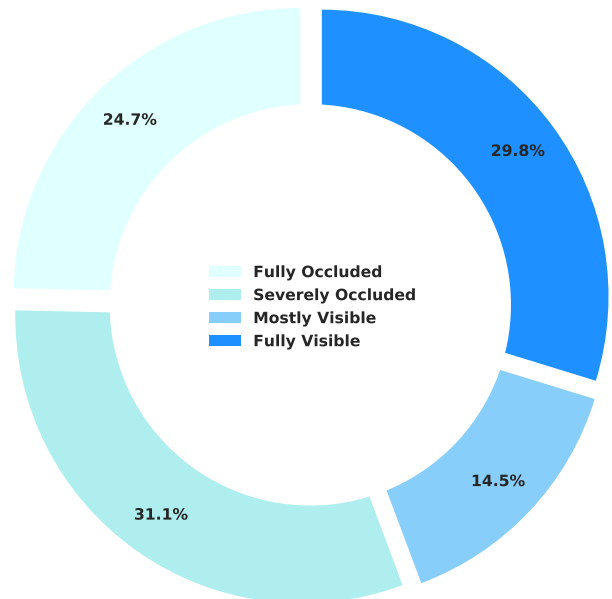


(b) Test Set Kernel Density Estimate

Fig. 6: The above plots show Kernel Density Estimates (KDEs) of the distribution of people around the robot, across the training and test splits of the dataset. Note that in close proximity of JackRabbit, people are evenly spread across all directions, but tend to be along the X-axis (with respect to the base frame) as the distance increases. This is due to the robot being driven along straight walkways when outdoors, and along corridors when indoors.



(a) Training Set



(b) Test Set

Fig. 7: We categorise occlusion (or lack thereof) into 4 distinct categories. The test set has a higher proportion of people that are completely occluded, making it more challenging for people tracking and detection. Approximately two thirds of the total number of boxes in both the train and test sets are more than 50% visible